Published in final edited form as:

*ACS Sens*. 2019 January 25; 4(1): 180–184. doi:10.1021/acssensors.8b01202.

# Emulsion Agglutination Assay for the Detection of Protein–Protein Interactions: An Optical Sensor for Zika Virus

**Qifan Zhang**[†,∇], **Lukas Zeininger**[†,∇], **Ki-Joo Sung**[‡], **Eric A. Miller**[‡], **Kosuke Yoshinaga**[†], **Hadley D. Sikes**[*,‡], **Timothy M. Swager**[*,†]

[†]Department of Chemistry and Institute for Soldier Nanotechnologies, Massachusetts Institute of Technology, 77 Massachusetts Avenue, Cambridge, Massachusetts 02139, United States

[‡]Department of Chemical Engineering, Massachusetts Institute of Technology, 77 Massachusetts Avenue, Cambridge, Massachusetts 02139, United States

## Abstract

A new class of Janus emulsion agglutination assay is reported for the detection of interfacial protein–protein interactions. Janus emulsion droplets are functionalized with a thermally stable, antigen binding protein rcSso7d variant (rcSso7d-ZNS1) for the detection of Zika NS1 protein. The emulsion droplets containing fluorescent dyes in their hydrocarbon and fluorocarbon phases intensify the intrinsic optical signal with the emission intensity ratio, which can be detected by a simple optical fiber. This assay provides an opportunity for the in-field detection of Zika virus and other pathogens with a stable, inexpensive, and convenient device.

## GRAPHICAL ABSTRACT:

[*]**Corresponding Authors:** tswager@mit.edu (T. M. Swager)., sikes@mit.edu (H. D. Sikes).
[∇]These authors contributed equally.

Supporting Information

The Supporting Information is available free of charge on the ACS Publications website at DOI: 10.1021/acssensors.8b01202.

General materials, detailed synthetic procedures. emulsion assay preparation, and production of rcSso7d variants (PDF)

The authors declare the following competing financial interest(s): A patent based on this technology has been filed.

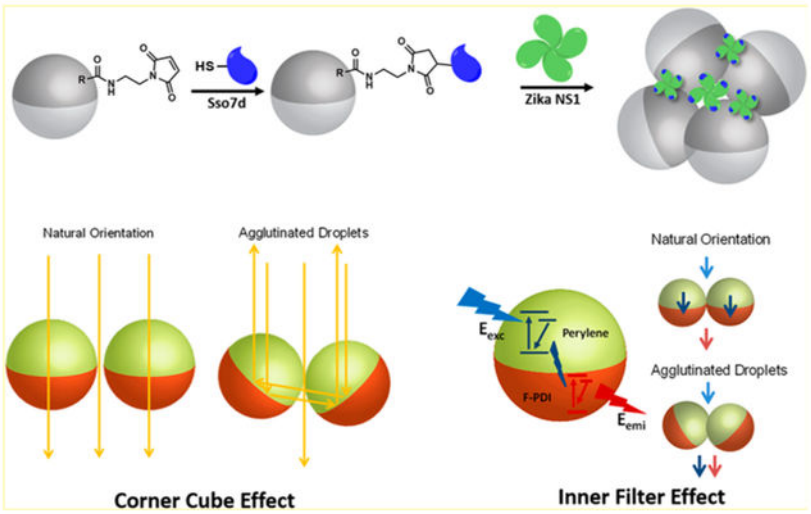


**Keywords**

carbohydrates; rcSso7d; emulsions; Zika virus; Janus particles; sensors

Zika is a vector-borne flavivirus that has emerged as a global health priority in recent years. Although Zika virus infections typically only cause mild febrile symptoms in adults, the virus can be passed from infected pregnant women to their fetuses and has been linked to severe birth defects such as microcephaly.[1] In addition, the Zika virus has been connected to neurological disorders in adults, including Guillain–Barré Syndrome.[1] No approved vaccines or treatments currently exist for the Zika virus; as a consequence, rapid accurate detection of Zika virus is essential to control epidemics and reduce the risk of these neurological complications. In recent years, many researchers have focused on developing assays for the detection of Zika virus, including polymerase chain reaction (PCR)[2] and antibody-based[3,4] assays. In addition, Zika virus detection using RNA amplification and CRISPR/Cas9 in rapid and low-cost sensors has been reported to be used in pandemic regions.[5] However, there is still a need for a sensing assay with high stability, lower cost, and less reliance on specialized instrumentation, which could become essential in areas with endemic transmission of Zika.

We have been investigating a new class of dynamic complex colloids[6] with demonstrated utility in sensing of antibodies[7] and bacteria.[8] Complex colloidal droplets composed of equal volumes of hydrocarbon and fluorocarbon liquid, exhibit dynamic morphological changes in response to external stimuli.[6] These droplets naturally align with gravity due to higher density of the fluorous phase,[8] and at the Janus state, the hydrocarbon phase and fluorocarbon phase are perfectly aligned hemispheres. The advantage of these colloids is the fact that the structured liquid phases have different refractive indices to produce directional optical properties[9] that are very sensitive to interfacial bioconjugation, molecular binding, and enzyme modification. In this work, we extend the applications of these droplets to the detection of the Zika virus by recognition of protein NS1, a nonstructural hexameric biomarker that plays a role in pathogenesis and immune evasion.[10] We detail herein an

agglutination assay for the detection of this analyte that is robust, low cost, and readily multiplexed.

Selectivity and sensitivity in our emulsion agglutination assay is determined by the specific binding activity to the target analyte and the translation of analyte binding to an agglutinated complex, which, in turn, changes optical transmission through a layer of emulsion droplets. To conjugate thiol containing receptor biomolecules, we employed a maleimide-functionalized polystyrene-*b*-poly(acrylic acid) (P1-MA) as the surfactant. Using this construction we conjugated variants of the hyperthermophilic binding protein, reduced-charged Sso7d (rcSso7d).[11] This selection is attractive as the rcSso7d protein is a viable replacement for antibodies in immunoassays, as a result of its intrinsic thermal and chemical stability, ease of large-scale biomanufacturing, and a versatile binding face. This protein scaffold can further be engineered to have high affinity for specific target proteins.[12,13] To optimize an agglutination assay, we began by using the streptavidin binding rcSso7d variant (rcSso7d-SA)[12] for the protein– protein recognition. In addition, we developed two novel optical transduction methods, which can be readily instrumented, for the quantification of the analyte. This optimization allowed for the efficient integration of the rcSso7d Zika NS1 binding variant (rcSso7d-ZNS1) into the assay format. The optimized system demonstrates a detection limit of 100 nM for the Zika NS1 protein. Emulsion droplet disposable assays based on the constructions presented herein have the advantage of thermally stable recognition elements, simple detection, and the avoidance of nucleic acid extractions that often require a trained technician.

Previously, gallic-acid-derived surfactants were used for droplet bioconjugation.[7] These surfactants exhibited good stability and displayed sensor behavior by triggering droplet morphology changes. However, the gallic-acid-derived surfactants did not have the anchoring strength necessary to hold multiple droplets together in an agglutination assay. The block copolymer anchor, polystyrene-*b*-poly(acrylic acid) (P1)) displayed the needed connection strength between the protein and droplets. The acrylic acid block in P1 was functionalized with maleimide-$NH_2$ to form P1-MA (Figure 1a). P1-MA was dissolved in the hydrocarbon phase and behaves as a hydrocarbon/water (H/W) interfacial active agent. This positions the maleimide group at the H/W interphase, enables the maleimide–thiol bioconjugation of cysteine-bearing proteins, and the production of protein-functionalized emulsion droplets.

To produce agglutination with the emulsion droplets, we have made use of protein–protein interactions, wherein the recognition protein rcSso7d is immobilized on the droplets. For this construction, the previously engineered rcSso7d-SA[12] was further genetically modified with a cysteine residue on the N-terminus for bioconjugation to the droplet. The cysteine modified rcSso7d-SA was then covalently linked to the hydrocarbon–water (H/W) interface via a maleimide–thiol conjugate addition reaction. The addition of the tetravalent streptavidin to the rcSso7d-SA functionalized droplets triggers agglutination by linking rcSso7d from different droplets together (Figure 1b). The agglutination was observed within 30 min of the addition of the streptavidin.

The amount of rcSso7d-SA conjugated to the droplet H/W interface is dependent upon droplet morphology during the reaction. To optimize the level of functionalization of rcSso7d-SA for agglutination, three initial morphologies (1) hydrocarbon-in-fluorocarbon-in-water (H/F/W), (2) Janus, and (3) fluorocarbon-in-hydrocarbon-in-water (F/H/W) were created by tuning the proportions of the continuous phase surfactants. As shown in Figure 2, each droplet initially has a different morphology and consequently a different surface area at the H/W interface for bioconjugation. After rcSso7d-SA functionalization, each droplet type was switched to the same morphology (Janus state) by exchanging the continuous phase surfactant solution in order to compare the relative agglutination responses. Streptavidin (0.36 $\mu$M) was added to agglutinate the Janus droplets. As shown in the micrographs in Figure 2, the droplets that were functionalized in a F/H/W morphology displayed a higher agglutination level. This result indicates that the increased surface area at the hydrocarbon/water interface facilitates the functionalization with rcSso7d and increases the agglutination sensitivity. Although a higher concentration of Tween 20 is used for the F/H/W morphology, the P1-MA molecule exhibits stronger surfactant behavior and effectively competes to partition at the H/W interface for an optimal maleimide–thiol conjugation reaction. Given the greater degree of agglutination achieved using droplets conjugated in the F/H/W morphology, this configuration was used for rcSso7d functionalization in all of the following studies.

Having established this emulsion assay for the detection of small quantities of streptavidin, we endeavored to create a quantitative optical readout of droplet agglutination. Multicompartment colloids have intrinsic optical properties, as a result of the differing refractive indices of the constituent phases.[9] Double emulsion droplets are tunable lenses with optical properties that vary with the droplet morphology.[14] The refractive index contrast and curvature of each interface contribute to the lenses' ability to focus or scatter.[9] The strong variations in the light transmission properties of Janus droplets before and after agglutination are displayed in the optical micrographs of Figure 2. Increases in the fraction of agglutinated (tilted) droplets causes more scattering of the incoming light, which can be measured in transmission or backscattering modes normal to the droplet layer. To produce a system displaying large optical effects, we chose a solvent combination with a relatively large refractive index (RI) contrast, such as diethylbenzene (RI = 1.49) for the hydrocarbon phase and HFE 7500 (RI = 1.29) for the fluorocarbon phase. Depending on the angle of the internal H/ F interface, the incoming light rays can intersect the internal H/F interface at angles below or above the critical angle: ($\theta$c = 60°). As a result, depending on the droplet's morphology and the refractive index contrast, the incoming light could undergo total internal reflection (TIR). In our agglutination sensing scheme, the selectors are selectively immobilized at the hydrocarbon/water interface, which leads to the aggregation of the high RI hydrocarbon phases. As a result of the surfaces and RI contrast, in the agglutinated state light can be backscattered in the upward direction, similar to a corner cube reflector (Figure 3b). In order to translate this light scattering effect into an applicable optical detection scheme, we positioned an optical fiber on top a droplet monolayer and recorded the light intensity (Figure 3a). For reproducibility and for creating a ratiometric readout of the degree of agglutination, we added a fluorescent dye (perylene; 1.5 mM) to the hydrocarbon phase and recorded the intensity ratio of the excitation light ($I_{exc}$) to the reference perylene

emission ($I_H$). Increased tilting of the droplets leads to an increase of the backscattered light intensity. Depending on the concentration of streptavidin and therefore the degree of agglutination, this optical sensor scheme provides a ratiometric signal for quantitative measurements with maximum intensity increase of up to 50% (Figure 3c).

In addition, we set out to create an additional purely fluorescent based sensor read-out of droplet agglutination. This method provides a more robust scheme, with the advantage of using multilayers of polydisperse droplets, more accurate ratiometric signals, and the possibility of multiplexing. In this scheme we dissolved a second emissive dye (F-PDI) in the fluorocarbon phase, which we recently demonstrated to show exclusive solubility in the fluorocarbon phase.[15] Changes in droplet alignment in response to streptavidin are quantified by recording the ratio of the emission from two dyes in the hydrocarbon and the fluorocarbon phase (Figure 4a). By targeted selection of the dyes, the emitted light of one of the dyes can be selectively attenuated via the inner filter effect depending on the orientation of the droplets. F-PDI exhibits absorption with a spectral. overlap with the emission of a high band gap (blue light emitting) perylene dye in the hydrocarbon phase. The overall emission of the emulsion will be dominated by the red fluorophore if the droplets are arranged in their gravity aligned fashion because the emitted light from the perylene dye collected by the optical fiber has to pass through the phase with the F-PDI dye before exiting the droplet. The degree of agglutination is accompanied by a continuous increase of the emission of the perylene dye, as a result of the decreased path length through the absorbing fluorocarbon phase (Figure 4b). As displayed in Figure 4c, the detection of the ratio of perylene ($I_H$) and F-PDI ($I_F$) emission provide for precise correlation with the level of agglutination, which can be used to quantify analyte concentration. Similar to the backscattering scheme described above, higher concentrations of streptavidin produce saturation of the light intensity ratio. Both methods show similar analyte sensitivity, which is indicated by the slope of the curve at low concentration.

The agglutination assay was then adapted for the detection of the polyvalent Zika NS1 protein using droplets conjugated to rcSso7d-ZNS1[13] via a cysteine at the N-terminus. The intensity curves reveal the sensitivity of the agglutination assay for Zika NS1 and the results are shown in Figure 5. As a result of the lower binding strength of the Zika NS1 to the rcSso7d-ZNS1, compared to the streptavidin to rcSso7d-SA, the reaction was equilibrated overnight, which allows for higher agglutination yields and the lowest limit of detection. The two optical schemes using the backscattering and inner filter effect are in agreement after normalization to the maximum (saturated) emission intensity, with a limit of detection of 100 nM. While conventional methods, such as DNA-, PCR-, or enzyme-based techniques can impart quite remarkable sensitivities, they require time-consuming enrichment steps, and complicated instruments, and thus prolonged sample-to readout times. Our emulsion droplets sensor illustrate an alternative and complementary mode of detecting Zika virus with the advantage of low cost, robustness and readiness with quantitative optical readouts. Considering the early development stage of this platform, it is likely that with new designs and hardware optimization significant improvements can be made in the future, either in the optical elements or the recognition schemes.

In conclusion, we have reported a novel agglutination assay for the detection of protein–protein interactions. We used Zika NS1 protein as a model study and we could sense at a limit of detection of 100 nM using two optical schemes that can be easily prototyped. A maleimide functionalized P1-MA polymer was used as the surface active agent to covalently link the hyperthermophilic rcSso7d protein to the surface of the droplets. The multivalent protein analyte Zika NS1 binds to surface-bound rcSso7d groups to cause droplet agglutination. Robust ratiometric signals to detect agglutination were developed by incorporating dyes in the droplets and detecting backscattered/emitted light, or multiple emissions modulated by an inner filter effect. This emulsion agglutination assay offers low power requirements without complicated labeling and nucleic acid handling. The assay is potentially suitable for use in remote locations without access to expensive equipment and trained personnel to identify Zika virus infections as well as other pathogenic species.

## ACKNOWLEDGMENTS

T.M.S. is grateful for funding from National Institutes of Health of General Medical Sciences (Grant No. GM095843). H.D.S. acknowledges support from the MIT Tata Center for Technology and Design, Singapore's National Research Foundation via the Singapore-MIT Alliance for Research and Technology (AMR IRG), the National Cancer Institute (Grant No. P30CCA14051), and MIT's Deshpande Center for Technological Innovation. L.Z. acknowledges support from the German Research Foundation (DFG, Grant No. ZE1121/ 1-1). K.S. thanks the National Science Foundation for a graduate research fellowship (Grant No. 1122374). K.Y. thanks the support from the Funai Overseas Scholarship.

## REFERENCES

(1). Musso D; Gubler DJ Zika Virus. Clin. Microbiol. Rev 2016, 29 (3), 487–524. [PubMed: 27029595]

(2). Lanciotti RS; Kosoy OL; Laven JJ; Velez JO; Lambert AJ; Johnson AJ; Stanfield SM; Duffy MR Genetic and Serologic Properties of Zika Virus Associated with an Epidemic, Yap State, Micronesia, 2007. Emerging Infect. Dis 2008, 14, 1232–1239. [PubMed: 18680646]

(3). Balmaseda A; Stettler K; Medialdea-Carrera R; Collado D; Jin X; Zambrana JV; Jaconi S; Cameroni E; Saborio S; Rovida F; Percivalle E; Ijaz S; Dicks S; Ushiro-Lumb I; Barzon L; Siqueira P; Brown DWG; Baldanti F; Tedder R; Zambon M; de Filippis AMB; Harris E; Corti D Antibody-Based Assay Discriminates Zika Virus Infection from Other Flaviviruses. Proc. Natl. Acad. Sci. U. S. A 2017, 114 (31), 8384–8389. [PubMed: 28716913]

(4). Lee KH; Zeng H Aptamer-Based ELISA Assay for Highly Specific and Sensitive Detection of Zika NS1 Protein. Anal. Chem 2017, 89 (23), 12743–12748. [PubMed: 29120623]

(5). Pardee K; Green AA; Takahashi MK; Braff D; Lambert G; Lee JW; Ferrante T; Ma D; Donghia N; Fan M; Daringer NM; Bosch I; Dudley DM; O'Connor DH; Gehrke L; Collins JJ Rapid, Low-Cost Detection of Zika Virus Using Programmable Biomolecular Components. Cell 2016, 165 (5), 1255–1266. [PubMed: 27160350]

(6). Zarzar LD; Sresht V; Sletten EM; Kalow J. a. ; Blankschtein D; Swager TM Dynamically Reconfigurable Complex Emulsions via Tunable Interfacial Tensions. Nature 2015, 518 (7540), 520–524. [PubMed: 25719669]

(7). Zhang Q; Scigliano A; Biver T; Pucci A; Swager TM Interfacial Bioconjugation on Emulsion Droplet for Biosensors. Bioorg. Med. Chem 2018, 26, 5307. [PubMed: 29691155]

(8). Zhang Q; Savagatrup S; Kaplonek P; Seeberger PH; Swager TM Janus Emulsions for the Detection of Bacteria. ACS Cent. Sci 2017, 3 (4), 309–313. [PubMed: 28470048]

(9). Nagelberg S; Zarzar LD; Nicolas N; Subramanian K; Kalow JA; Sresht V; Blankschtein D; Barbastathis G; Kreysing M; Swager TM; Kolle M Reconfigurable and Responsive Droplet-Based Compound Micro-Lenses. Nat. Commun 2017, 8, 14673. [PubMed: 28266505]

(10). Brown WC; Akey DL; Konwerski JR; Tarrasch JT; Skiniotis G; Kuhn RJ; Smith JL Extended Surface for Membrane Association in Zika Virus NS1 Structure. Nat. Struct. Mol. Biol 2016, 23 (9), 865–867. [PubMed: 27455458]

(11). Traxlmayr MW; Kiefer JD; Srinivas RR; Lobner E; Tisdale AW; Mehta NK; Yang NJ; Tidor B; Wittrup KD Strong Enrichment of Aromatic Residues in Binding Sites from a Charge-Neutralized Hyperthermostable Sso7d Scaffold Library. J. Biol. Chem 2016, 291 (43), 22496–22508. [PubMed: 27582495]

(12). Miller EA; Traxlmayr MW; Shen J; Sikes HD Activity-Based Assessment of an Engineered Hyperthermophilic Protein as a Capture Agent in Paper-Based Diagnostic Tests. Mol. Syst. Des. Eng 2016, 1 (4), 377–381.

(13). Miller EA; Baniya S; Osorio D; Al Maalouf YJ; Sikes HD Paper-Based Diagnostics in the Antigen-Depletion Regime: High-Density Immobilization of RcSso7d-Cellulose-Binding Domain Fusion Proteins for Efficient Target Capture. Biosens. Bioelectron 2018, 102, 456–463. [PubMed: 29182928]

(14). Zarzar LD; Kalow JA; He X; Walish JJ; Swager TM Optical Visualization and Quantification of Enzyme Activity Using Dynamic Droplet Lenses. Proc. Natl. Acad. Sci. U. S. A 2017, 114 (15), 3821–3825. [PubMed: 28348236]

(15). Yoshinaga K; Swager T Fluorofluorescent Perylene Bisimides. Synlett 2018, 29, 2509.

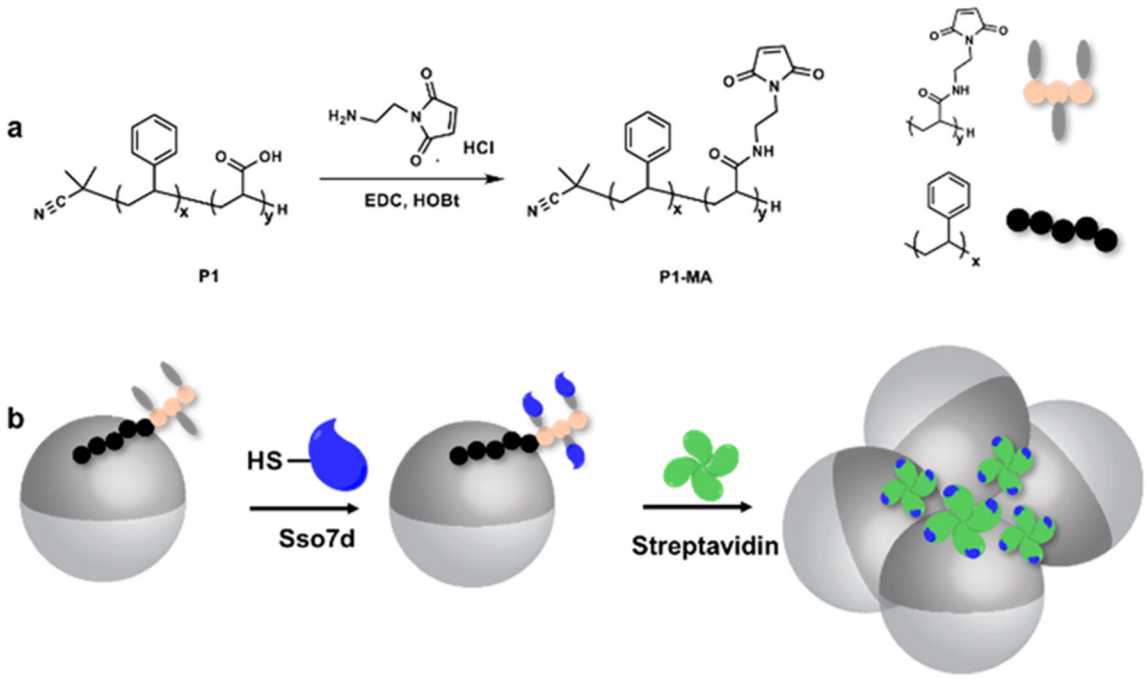


**Figure 1.**

Functionalization of the droplets with the polymer surfactant. (a) Synthesis of maleimide-functionalized surfactant P1-MA from a polystyrene-*b*-poly(acrylic acid) polymer. (b). Bioconjugation of rcSso7d to the droplet H/W interface via maleimide–thiol chemistry. The addition of streptavidin to the rcSso7d-functionalized droplets assay cause agglutination. The hydrocarbon phase is shown in dark gray for display purposes. The scheme is illustrative and is not to scale.

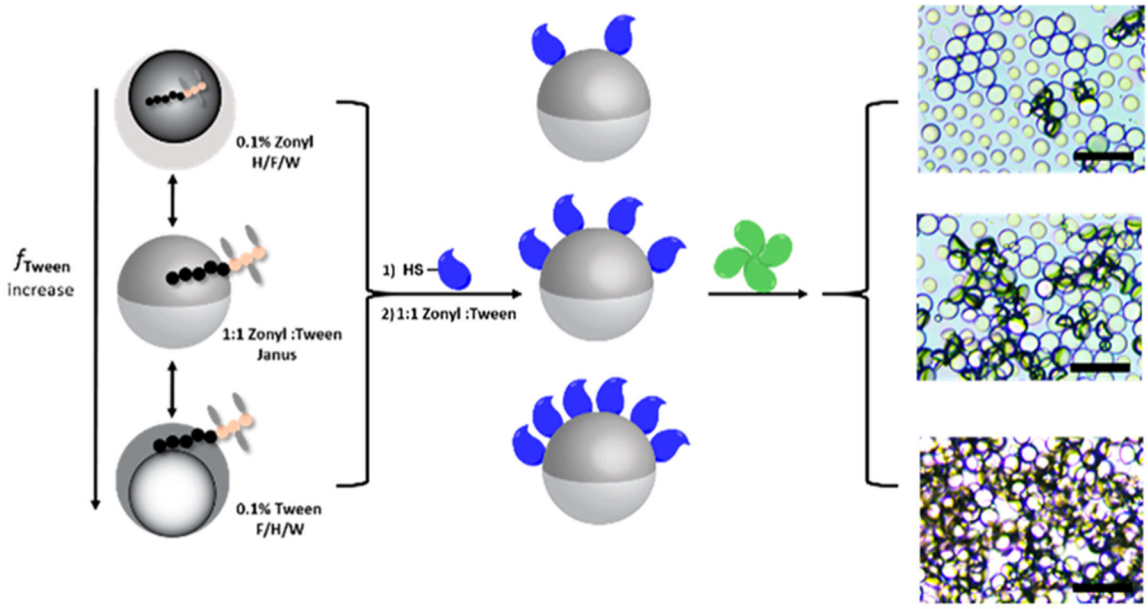


**Figure 2.**

Droplets starting at different morphologies, namely, H/F/W, Janus, and F/H/W functionalized with cysteine engineered rcSso7d. The continuous phase was exchanged to tune the morphology into the Janus format, followed by the addition of 10 $\mu$L of 1 mg $mL^{-1}$ (0.36 $\mu$M) streptavidin. Note that a higher degree of agglutination is observed with droplets prepared at the higher Tween 20 concentrations. The scale bars in the optical micrographs are 100 $\mu$m.

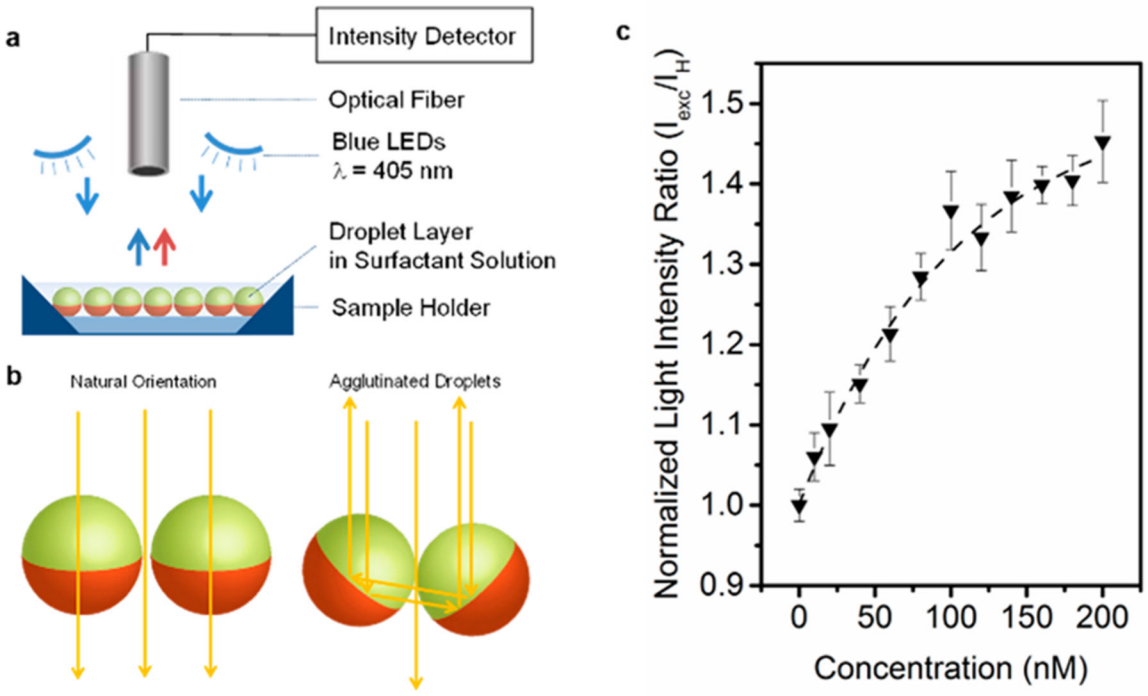


**Figure 3.**

Optical detection using the backscattering scheme. (a) Experimental setup with both excitation and detection source from the top of the emulsion layer. (b) Scheme showing the backscattering of the light with naturally oriented Janus droplets and agglutinated droplets. c. Optical measurement with the intensity ratio $I_{exc}/I_H$ in correlation with the streptavidin concentration.

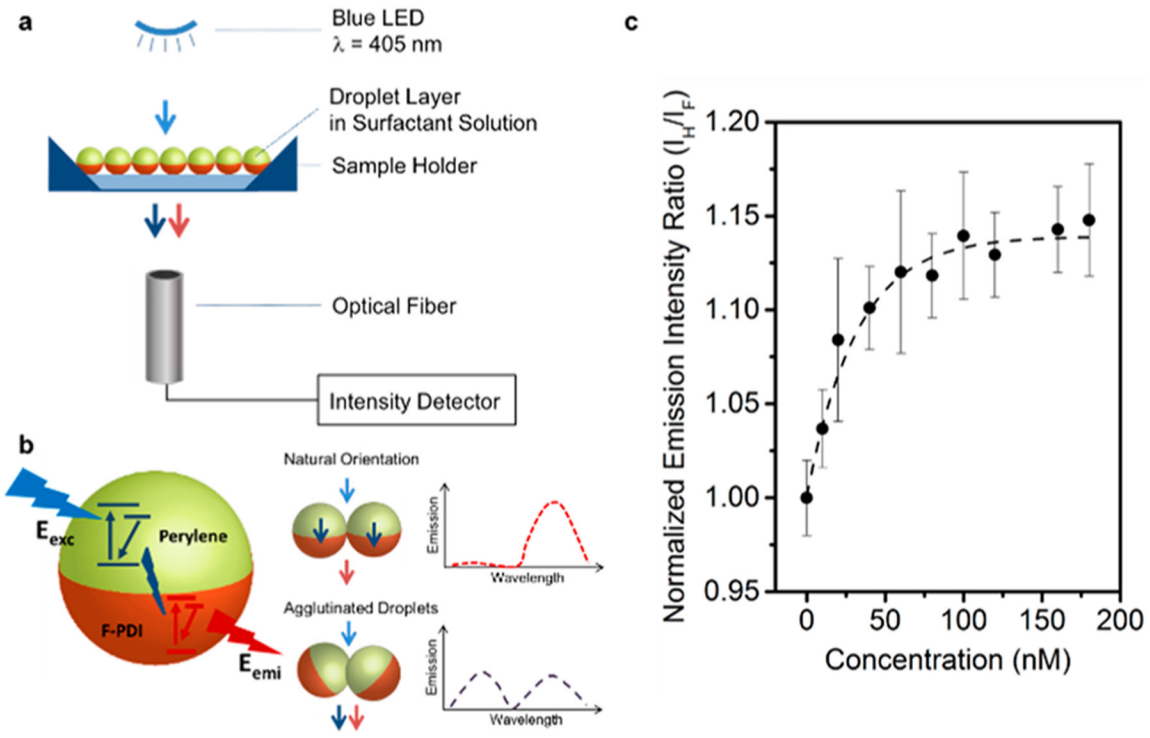


**Figure 4.**

Optical scheme using the inner filter effect. (a) Experimental setup with the optical fiber at the bottom of the emulsion layer. (b) Scheme showing the mechanism of the attenuated emission of the perylene dye, which is dependent on the orientation of the droplets. (c) Experimental data showing the optical detection of the emission intensity ratio $I_H/I_F$ in correlation of the streptavidin concentration.

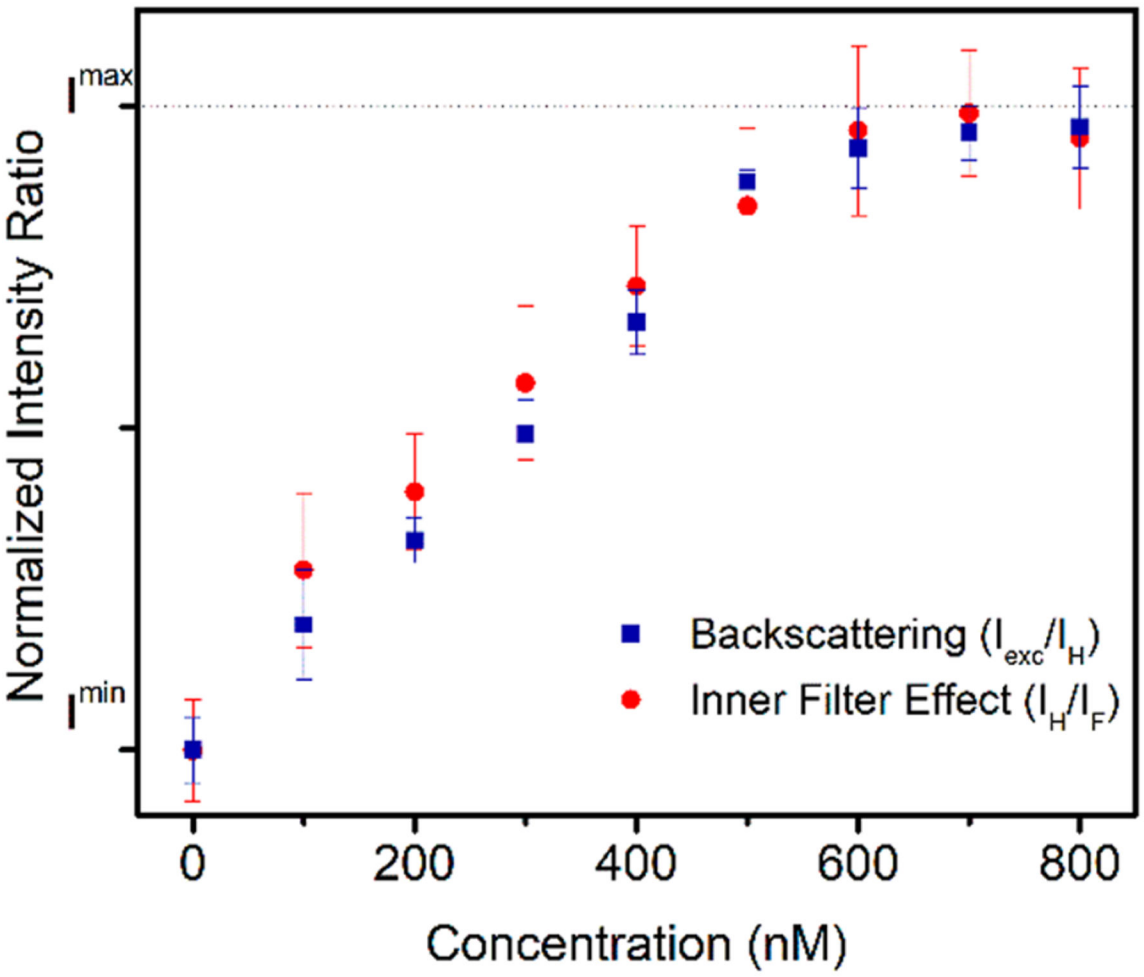


**Figure 5.**
Zika detection using the backscattering and the inner filter effect.